The Meteoritical Society

Meteoritics & Planetary Science 42, Nr 10, 1817–1829 (2007)
Abstract available online at http://meteoritics.org

The formation of eucrites: Constraints from metal-silicate partition coefficients

A. HOLZHEID[1†*] and H. PALME[2]

[1]Institut für Mineralogie, Westfälische Wilhelms-Universität Münster, Corrensstrasse 24, 48149 Münster, Germany
[2]Institut für Geologie und Mineralogie, Universität zu Köln, Zülpicher Strasse 49b, 50674 Köln, Germany
[†]Present address: Institut für Geowissenschaften, Universität Kiel, 24098 Kiel, Germany

[*]Corresponding author. E-mail: holzheid@min.uni-kiel.de

(Received 29 July 2006; revision accepted 02 April 2007)

Abstract–This study explores the controls of oxygen fugacity and temperature on the solubilities of Fe, Ni, Co, Mo, and W in natural eucritic liquids to better constrain the formation of eucritic melts. The solubilities of all five elements in molten silicate in equilibrium with FeNiCo-, FeMo-, and FeW-alloys increase with increasingly oxidizing conditions and decrease with decreasing temperatures. In applying these data to formation scenarios of the eucrite parent body, we find that the siderophile element abundances in eucrites (meteoritic basalts) cannot be explained by a single-step partial-melting process from a chondritic, metal-containing source. The Ni content of the partial melt is too high, and the W and Mo contents are too low compared to the abundances in eucritic meteorites. But Fe, Ni, and Co concentrations in eucrites can be modeled by metal-silicate equilibrium during more or less complete melting of the eucrite parent body with subsequent fractional crystallization of olivine and orthopyroxene. However, the computed values of Mo are still too low and those of W too high when compared with Mo and W abundances in eucritic meteorites. One possibility is that the Mo and W partition coefficients strongly depend on pressure, although the howardite-eucrite-diogenite (HED) parent body only had a minimal pressure gradient (maximum interior pressure = 0.1 GPa). Alternatively, sulfides may have played some role in establishing Mo abundances.

INTRODUCTION

Eucrites are the most common type of achondrites, i.e., a class of fine-grained, brecciated stony meteorites that formed as basaltic flows on their asteroid-sized parent body, the eucrite parent body (EPB). The meteorites consist mostly of Ca-rich plagioclase and pigeonite pyroxene (for detailed petrographic description, see BVSP 1981 and references therein). Variations in the bulk chemical composition among the eucrites are used to define four distinctive groups: main group eucrites, Stannern trend eucrites, Nuevo Laredo trend eucrites, and cumulate eucrites. Only a few eucrites do not fit into one of the above groups; these are called anomalous eucrites (see BVSP 1981 for more detail). Related to eucrites are diogenites, which are primarily composed of cumulate pyroxenes and howardites, achondrite breccias containing fragments of eucrites, and diogenites. All three types of achondrites are petrogenetically related and should therefore come from a single planet or planetesimal, the howardite-eucrite-diogenite (HED) parent body (Takeda et al. 1976). This idea is supported by similarities in O isotopes of all three types of achondrites (e.g., Clayton and Mayeda 1996; Wiechert et al. 2004). Asteroid 4 Vesta is believed to be the HED parent body as first proposed by McCord et al. (1970) and Consolmagno and Drake (1977). Later findings by Binzel and Xu (1993) have strengthened this suggestion. Chemical compositions and mineralogical phases of eucritic meteorites and estimated composition of the EPB permit questions addressing the formation of the eucritic basalts. Based on incompatible lithophile trace element abundances in HED meteorites, two general classes of models for the formation of these meteorites were suggested. The first type of hypothesis, initially proposed by Stolper (1975), explains the main group and Stannern trend eucrites by variable degrees of partial melting of a chondritic, metal-containing source region. This model was later modified by Stolper (1977) and Consolmagno and Drake (1977), and revisited by Jurewicz et al. (1993). According to the second hypothesis, eucrites are the result of fractional crystallization of an EPB-magma ocean (e.g., Mason 1962; McCarthy et al. 1973; Ikeda and Takeda 1985; Warren 1985; Warren and Jerde 1987; Bartels and Grove 1991; Grove and Bartels 1992;

Ruzicka et al. 1997a, 1997b). Some authors combine elements of both models, e.g., Hewins and Newsom (1988) and Righter and Drake (1996, 1997). Righter and Drake (1997) designed a five-stage model for core formation in the EPB and the formation of eucrites. In their model, the HED meteorites are formed as part of a simple and continuous crystallization sequence starting from a largely molten eucrite parent body and followed by equilibrium crystallization at the beginning and later leading to fractional crystallization after the melt had separated from crystals by gravitational forces in the Vesta magma ocean. However, none of the models is able to account for all of the compositional variations seen in the various types of eucrites and diogenites.

In general, knowledge about the partitioning of siderophile elements between coexisting metal, sulfide, and silicate phases is one of the prerequisites for a quantitative understanding of differentiation processes in planetary bodies. Formation of metal or metal-sulfide cores in planets will remove siderophile (metal-seeking) and/or chalcophile (sulfide-seeking) elements from the silicate protomantle into the separating metallic phase. Absolute and relative abundances of siderophile and chalcophile elements in the silicate mantle after cessation of core formation provide information about the type and extent of the core formation process when compared with calculated abundances from experimentally determined metal-silicate and sulfide-silicate partition coefficients (see, e.g., Walter et al. 2000 for more detail).

The existing set of metal-silicate partition data is limited with respect to temperature and melt composition. The purpose of the present experimental investigation therefore is to study the solubilities of siderophile elements within an extended temperature interval and with aliquots of the eucrite Millbillillie as silicate starting material. In this way, uncertainties arising from compositional differences between experimental charges and natural samples are minimized. These new data are then used to derive additional constraints on formation scenarios of meteoritic basalts. Because of the low pressure in the interior of Vesta and similarly sized asteroids (maximum pressure = 0.1 GPa), experiments at one atmosphere pressure are sufficient to constrain core formation and silicate differentiation.

EXPERIMENTAL TECHNIQUES AND RESULTS

Methodology

Aliquots of the eucrite Millbillillie were used as silicate starting material. A total of about 1.5 g of Millbillillie was finely ground by hand in an agate mortar under acetone. Aliquots (10–35 mg) of this batch were then equilibrated with either a commercially available Fe-, Co-, and Ni-bearing alloy (Fe 54 wt%, Co 17%, Ni 29%), pure Mo metal, or pure W metal (all metals from Goodfellow). The experimental setup was similar to that used for the determination of Ni, Co, Fe, and Mo solubilities by Holzheid et al. (1994) and Holzheid and Palme (1996). All experiments were conducted in a vertical tube furnace at one atmosphere. The oxygen fugacity was controlled by gas mixtures of CO and CO_2. A $Pt_{94}Rh_6/Pt_{70}Rh_{30}$ thermocouple and a CaO-Y_2O_3-stabilized ZrO_2 solid electrolyte sensor were employed for measuring temperature and oxygen fugacity. Experiments at temperatures below the melting point of the metal were done by a loop technique, whereby the powdered silicate starting materials mixed with an organic glue were inserted into metal loops (ID 2 mm; see Borisov et al. 1994 for details). For FeNiCo experiments at temperatures above 1450 °C, powdered silicates and metal powders were mixed in a ratio of approximately 50/50 (by mass) and inserted into small corundum crucibles (length 10 mm, ID 8 mm), causing some enrichment of Al_2O_3 in the silicate liquid during the experiments Mill-8 and Mill-9. Loops and/or crucibles were then equilibrated under different oxygen fugacities and temperatures. Run durations varied between 6 h at run temperatures of 1600 °C and 4 days at 1211 °C. Because of the comparatively large diameter of the working tube of the furnace (ID 57 mm), several metal loops and/or corundum crucibles could be simultaneously heated. This is indicated by identical run numbers for certain samples (Table 2). Holzheid et al. (1994) demonstrated attainment of equilibrium by homogeneous distribution of the elements in silicates and metals and by several reversed experiments (see Holzheid et al. 1994 for details). Samples were quenched to glass by withdrawing them from the hot zone to the top of the furnace. After separation from the metal phase, glass samples were polished to remove possible contamination with loop metal. Glass samples from the alumina crucible experiments were separated by crushing the glass-containing crucible and hand-picking individual glass fragments. Fragments adhering to the crucible were avoided.

Concentrations of Fe, Co, Ni, Mo, and W in glasses were determined by instrumental neutron activation analysis (INAA). Irradiations were performed in the core of the TRIGA-reactor of the Institut für Kernchemie at the Universität Mainz with a neutron flux of $4.2 \cdot 10^{12}$ n $\cdot$ cm^{-2} sec^{-1} and a duration of irradiation of 6 h. Because of the higher fast neutron flux in the core of the reactor, the sensitivities for the elements Fe, Co, Ni, Mo, and W were increased by factors of about 5 (Fe), 4 (Co), 20 (Ni), 6 (Mo), and 3 (W) compared to irradiations in the carousel of the TRIGA-reactor. Samples were counted on large volume Ge(Li) detectors at the Universität Köln. Decays of ^{59}Fe (1099.3, 1291.6 keV, $\tau_{½}$ = 45 days), ^{60}Co (1173.2, 1332.5 keV, $\tau_{½}$ = 5.3 yr), ^{58}Co (for Ni, 810.5 keV, $\tau_{½}$ = 71 h), ^{99}Tc (for Mo, 140.5 keV, $\tau_{½}$ = 66 h), and ^{187}W (479.5, 685.7 keV, $\tau_{½}$ = 24 h) were registered.

Table 1. Concentrations of Fe, Co, and Ni in selected eucrites, analyzed by instrumental neutron activation technique.

	Weight (mg)	Fe (%)	s.d.	Co (ppm)	s.d.	Ni (ppm)
Millbillillie	88.1[a]	14.44	5	6.01	5	<3.46
Millbillillie	165[a]	15.23	5	6.62	5	<10.5
Millbillillie	avg.[b]	14.95	5	6.41	5	<6.98
Stannern	188	14.51	5	3.70	5	<4.66
Bouvante	206	15.57	5	2.83	5	<5.20

[a]Aliquots of Millbillillie, separately ground to powder.
[b]Weighted average of the two aliquots; s.d. = standard deviations in rel%.

The major elements of the silicate glasses and corresponding alloys were analyzed by electron microprobe. A beam current of 20 nA, an accelerating voltage of 15 keV, and counting times of 20 s were employed for silicate measurements. A beam current of 20 nA, an accelerating voltage of 12 keV, and counting times of 30 s were employed for metal measurements.

Results

Concentrations of Fe, Co, and Ni in Selected Eucrites

First we re-examined the abundances of Fe, Co, and Ni in eucrites as the paper's attempt is to explain the concentrations of these elements in eucrites. Aliquots of the eucrites Millbillillie, Stannern, and Bouvante were analyzed by INAA. The samples were irradiated in the core of the TRIGA-reactor of the Institut für Kernchemie at Universität Mainz. Procedures of counting the samples on large volume Ge(Li) detectors at Universität Köln are as described in the Experimental Techniques and Results section of our paper. The revised Fe, Co, and Ni concentrations in Millbillillie, Stannern, and Bouvante are listed in Table 1. Concentrations of Fe agree within 2-sigma and better when compared to eucrite compositions given in Barrat et al. (2000, Table 3 therein), while our Co concentrations are lower by factors of 1.2 (Millbillillie), 2.1 (Stannern), and 1.5 (Bouvante). The agreement of Co concentrations in Stannern and Bouvante with data from Mittlefehldt and Lindstrom (2003) is slightly better. Our Co concentrations are lower by factors of 1.6 (Stannern) and 1.1 (Bouvante). As our Ni concentrations are upper limits, the Ni contents in Millbillillie and Stannern (this work) are consistent with Warren (1999) and Barrat et al. (2000), while a lower Ni content (as upper limit) in Bouvante was found in our study. Compilations of major and trace element abundances of noncumulate eucrites (Kitts and Lodders 1998; Barrat et al. 2000) show in general fair agreement between calculated normative (CIPW) compositions and observed mineral abundances in noncumulate eucrites. The use of Millbillillie as representative silicate starting material of eucrites in our experiments is therefore justified.

Partition Behavior of Fe, Co, Ni, Mo, and W Between Metal and Millbillillie

Experimental parameters (temperature, run duration, and oxygen fugacity) and chemical compositions of the coexisting phases (alloy and silicate glass) in our experimental products are presented in Tables 2 and 3.

Depending on the oxygen fugacity that prevailed during the experiments, some of the FeO in the silicate was reduced to Fe and partitioned as Fe into the metal phase or, as in experiments with FeCoNi alloys as starting metal, some of the metallic Fe was oxidized and partitioned as Fe oxide into the silicate phase. These reactions are responsible for the variations in FeO in the post-run silicate charges. Contributions of reduced Co, Ni, Mo, or W oxides of the eucritic silicate to the metal phases were negligible in all cases. The Co, Ni, Mo, or W concentration of the silicate increased by oxidation reactions of the metal that coexisted with the silicate liquid. In all experiments with initially pure Mo and W metal phases, some of the FeO in the silicate was reduced to Fe and partitioned into the metal phase, producing either FeMo or FeW metal alloys.

The siderophile element distribution coefficients between coexisting metal and silicate phases were recalculated to solubilities of pure metals in silicate liquids (for more details, see Holzheid and Palme 1996). For example, the Ni distribution between $Fe_{54}Co_{17}Ni_{29}$ alloy and Millbillillie silicate is recalculated to the equilibrium between pure Ni metal and silicate liquid by using the activity coefficient of Ni in the $Fe_{54}Co_{17}Ni_{29}$ alloy. This procedure allows direct comparison of results of all Ni experiments available in the literature. Equation 3 in Holzheid and Palme (1996) was used for the calculation of the solubilities between pure metal phase of interest and Millbillillie silicate. Activity coefficients of Fe (γ_{Fe}), Co (γ_{Co}), and Ni (γ_i), in FeCoNi alloys were calculated using the interaction parameters of ternary FeCoNi solution derived from excess molar free energies of the solutions, G^{xs}, obtained from Guillermet (1989) (see Holzheid and Palme 1996 for details). Activity coefficients of Mo (γ_{Mo}) and W (γ_W) in FeMo and FeW alloys were calculated using Equation 20 (FeMo) and Table 4 (FeW) in Ichise et al. (1980) and Ueshima et al. (1984), respectively.

Metal-silicate partition coefficients $D_{sol}(M/S)$ calculated from solubilities as described above are listed in Table 2 and plotted as function of oxygen fugacity at isothermal conditions of 1400 °C in Fig. 1 (Ni-, Co-, Fe-D_{sol}[M/S]) and Fig. 2 (Mo-, W-D_{sol}[M/S]). Closed symbols correspond to experiments with Millbillillie as silicate starting material. Partition coefficients obtained in earlier studies (Holzheid et al. 1994; Holzheid and Palme 1996) are plotted as open symbols (FeO-free system) and gray symbols (FeO-containing system). Best-fit lines (solid lines) are based on all experimental data (i.e., experiments with Millbillillie and earlier experiments in Fe-free and Fe-containing systems). The slope of the least square regressions is a function of the

Table 2. Run parameters, element concentrations in metal phases, and metal-silicate partition coefficients.

	T (°C)	Time (h)	log fO_2	ΔIW	Metal Fe (%)	Metal Co (%)	Metal Ni (%)	Total	D_{sol}(M/S) Fe	D_{sol}(M/S) Co	D_{sol}(M/S) Ni
Mill-4	1401	48	−8.79	IW + 0.91	53.1(1)	16.61(1)	28.6(1)	98.3	1.14	12.1	258
Mill-10	1401	60.5	−9.59	IW + 0.11	41.9(1)	21.7(1)	34.0(1)	97.6	1.44	26.5	460
Mill-1	1400	48	−9.62	IW + 0.09	40.1(1)	21.9(1)	36.3(1)	98.3	1.50	37.8	648
Mill-2	1400	48	−10.64	IW − 0.93	46.8(1)	24.6(1)	27.6(1)	99.0	3.20	181	2360
Mill-12	1400	70.5	−10.73	IW − 1.02	54.1(1)	16.1(2)	28.9(2)	99.1	4.35	118	3190
Mill-3	1399	48	−11.79	IW − 2.07	60.6(1)	14.2(1)	24.1(1)	98.9	13.6	419	6710
Mill-5	1397	48	−11.93	IW − 2.19	56.6(1)	15.4(1)	26.3(1)	98.3	16.0	805	15,700
Mill-11	1400	60	−12.60	IW − 2.89	64.4(3)	12.5(5)	21.8(5)	98.7	53.0	1100	
Mill-14	1211	96	−12.83	IW − 1.04	61.1(2)	13.7(2)	24.3(3)	99.1	7.33	300	6000
Mill-6	1296	49	−11.78	IW − 0.99	64.3(2)	12.4(1)	23.0(1)	99.7	5.01	158	2890
Mill-2	1400	48	−10.64	IW − 0.93	46.8(1)	24.6(1)	27.6(1)	99.0	4.48	129	2360
Mill-12	1400	70.5	−10.73	IW − 1.02	54.1(1)	16.1(2)	28.9(2)	99.1	4.81	148	3190
Mill-9	1501	21	−9.85	IW − 1.07	50.4(1)	18.9(1)	29.4(1)	98.7	3.96	106	1320
Mill-8	1603	6	−9.04	IW − 1.09	51.9(1)	18.9(1)	29.5(2)	100.3	4.32	101	1280

	T (°C)	Time (h)	log fO_2	ΔIW	Metal Fe (%)	Metal W (%)	Metal Mo (%)	Total	D_{sol}(M/S) W	D_{sol}(M/S) Mo
Mill-10	1401	60.5	−9.59	IW + 0.11	0.086(2)	99.7(1)		99.8	2.20	
Mill-10	1401	60.5	−9.59	IW + 0.11	0.264(2)		99.4(1)	99.7		276
Mill-11	1400	60	−12.60	IW − 2.89	0.682(1)	97.1(1)		97.8	436	
Mill-11	1400	60	−12.60	IW − 2.89	5.44(1)		94.5(1)	99.9		100,400

The oxygen fugacity (fO_2) is from zirconia oxygen-sensor measurements. ΔIW: oxygen fugacity values expressed relative to the iron-wüstite (IW) buffer. All concentrations are given in wt% as determined by electron microprobe analyses. Numbers in parentheses are 1σ deviations. The entry should be read 53.1 wt% ± 0.1 wt%. D_{sol}(M/S): solubility partition coefficients (see text for detail).

Table 3. Element concentrations in silicate phases.

	SiO_2	TiO_2	Al_2O_3	Cr_2O_3	FeO	MnO	MgO	CaO	Na_2O	P_2O_5	Co	Ni	Total
Mill-4	25.8(30)	0.301(141)	6.29(367)	0.229(123)	55.3(32)	1.22(15)	4.16(111)	4.54(199)	0.008(13)	0.012(15)	10,940(5)	1100(10)	99.0
Mill-10	37.1(2)	0.470(25)	10.3(1)	0.251(43)	31.4(3)	0.912(84)	5.41(7)	7.83(6)	0.012(12)	0.007(8)	6896(5)	771(7)	94.5
Mill-1	42.0(2)	0.548(21)	11.5(1)	0.281(84)	27.0(4)	0.879(63)	6.17(9)	8.89(7)	0.024(15)	0.009(11)	4943(5)	585(5)	97.8
Mill-2	49.5(2)	0.648(21)	14.1(1)	0.319(78)	15.0(2)	0.953(104)	7.06(3)	10.5(1)	0.015(13)	0.002(6)	1129(5)	124(8)	98.2
Mill-12	50.3(4)	0.630(20)	14.0(1)	0.330(71)	14.2(3)	0.912(63)	7.21(6)	10.6(1)	0.018(10)	0.014(19)	1085(5)	88.6(20)	98.4
Mill-3	54.9(2)	0.744(17)	15.7(1)	0.347(75)	5.06(13)	0.477(82)	8.17(6)	12.3(1)	0.013(14)	0.003(4)	261(5)	34.0(50)	97.7
Mill-5	54.8(4)	0.731(21)	16.2(1)	0.313(44)	3.80(9)	0.447(74)	7.97(7)	12.5(1)	0.012(12)	0.008(13)	150(5)	16.1(50)	96.8
Mill-11	57.0(2)	1.04(2)	17.0(1)	0.285(21)	1.15(6)	0.069(25)	8.73(6)	12.4(3)	0.004(4)	0.001(2)	85.3(5)	<d.l.	98.1
Mill-14	53.9(3)	0.656(25)	14.9(1)	0.383(35)	8.42(17)	1.17(8)	7.67(4)	11.3(1)	0.151(23)	0.008(11)	457(5)	37.0(25)	98.6
Mill-6	49.2(2)	0.644(27)	14.0(1)	0.359(58)	15.2(2)	0.957(73)	6.85(11)	10.5(1)	0.023(1)	0.012(18)	789(5)	72.2(9)	97.7
Mill-2	49.5(2)	0.648(21)	14.1(1)	0.319(78)	15.0(2)	0.953(104)	7.06(3)	10.5(1)	0.015(13)	0.002(6)	1129(5)	124(8)	98.2
Mill-12	50.3(4)	0.630(20)	14.0(1)	0.330(71)	14.2(3)	0.812(63)	7.21(6)	10.6(1)	0.018(10)	0.014(19)	1085(5)	88.6(20)	98.4
Mill-9	34.5(1)	0.440(20)	36.0(1)	0.083(41)	15.7(1)	0.552(69)	3.87(5)	7.45(5)	0.186(23)	0.005(7)	1776(5)	227(7)	98.9
Mill-8	30.3(11)	0.395(13)	41.6(10)	0.149(66)	14.5(2)	0.529(90)	4.45(10)	6.62(22)	0.198(29)	0.016(21)	1872(5)	236(8)	98.9
	SiO_2	TiO_2	A_2O_3	Cr_2O_3	FeO	MnO	MgO	CaO	Na_2O	P_2O_5	W	Mo	Total
Mill-10	51.9(21)	0.374(20)	18.8(6)	0.187(48)	12.0(2)	0.532(61)	9.41(6)	6.08(9)	0.021(18)	0.028(29)	448,200(5)	99.7	95.8
Mill-10	47.4(2)	0.621(21)	13.1(1)	0.291(73)	16.4(3)	0.818(93)	6.83(6)	9.92(7)	0.016(15)	0.004(6)		3603(5)	98.7
Mill-11	55.1(3)	0.875(31)	17.9(1)	0.264(59)	1.59(5)	0.040(47)	9.05(7)	13.9(7)	0.007(11)	0.007(15)	2260(5)		99.7
Mill-11	54.5(3)	0.881(23)	18.8(1)	0.221(67)	1.28(8)	0.077(38)	9.19(9)	14.5(1)	0.018(12)	0.010(11)		9.57(5)	95.8

All major element concentrations are given in wt% as determined by electron microprobe analyses. Concentrations of Ni, Co, Mo, and W are obtained by instrumental neutron activation and are given in ppm. Numbers in parentheses are 1σ deviations. The entry should be read 25.8 wt% ± 3.0 wt% for all major elements. The entry reflects 1σ deviations in rel% for Ni, Co, Mo, and W. Variations in Al_2O_3 are due to the change of container material, i.e., metal capsule at experiments up to 1400 °C and alumina crucibles at T > 1500 °C.

Table 4a. Fit coefficients for metal-silicate partition coefficients as function of oxygen fugacity.

	No.	c_1	c_2	R^2	Formal valence
Ni	52	–1.52 ± 0.29	–0.45 ± 0.03	0.85	1.80 ± 0.12
Co	52	–3.06 ± 0.15	–0.49 ± 0.01	0.96	1.96 ± 0.04
Fe	50	–4.33 ± 0.09	–0.47 ± 0.01	0.98	1.88 ± 0.04
$Mo^{(1)}$	10	–5.87 ± 0.67	–0.92 ± 0.06	0.97	3.68 ± 0.24
$Mo^{(2)}$	9	–9.76 ± 0.40	–1.27 ± 0.04	0.99	5.08 ± 0.16
W	8	–7.92 ± 0.90	–0.87 ± 0.08	0.96	3.48 ± 0.32

Least square regressions are based on experiments with Millbillillie (this study), experiments in Fe-free system (Ni, Co, Mo: Holzheid et al. 1994; W: Ertel et al. 1996), and Fe-containing system (Ni, Co, Fe: Holzheid and Palme 1996; Mo: unpublished data). All data are for 1400 °C. Fit parameters are for log $D_{sol}(M/S) = c_1 + c_2 \cdot \log fO_2$. No.: number of observations. Formal valence = $4 \cdot c_2$. $Mo^{(1)}$: Mo-D_{sol}(M/S) at oxygen fugacities more reduced than 1 log unit below the Fe-FeO equilibrium (IW-1) are used for least square regression. $Mo^{(2)}$: Mo-D_{sol}(M/S) at oxygen fugacities more oxidized than IW-1 are used for least square regression.

Table 4b. Fit coefficients for metal-silicate partition coefficients as function of temperature at IW-1 (i.e., one log-unit below iron-wüstite buffer).

	#	c_3	c_4	R^2
Ni	35	0.46 ± 0.22	0.48 ± 0.04	0.82
Co	36	0.65 ± 0.21	0.27 ± 0.04	0.61
Fe	21	No T-dependence as D_{sol}(M/S) is recalculated to IW-1		
Mo	12	0.71 ± 0.70	0.53 ± 0.12	0.66
W	4	–1.26 ± 0.75	0.47 ± 0.13	0.87

Least square regressions are based on experiments with Millbillillie (this study), experiments in Fe-free system (Ni, Co, Mo: Holzheid et al. 1994; W: Ertel et al. 1996), and Fe-containing system (Ni, Co, Fe: Holzheid and Palme 1996). Data cover a temperature range from 1211 to 1600 °C. Fit parameters are for log $D_{sol}(M/S) = c_3 + c_4 \cdot 10^4/T$ [K]. #: number of observations.

valence state of the metal oxide (formal valence = $-4 \cdot$ slope of the regressions) (see Holzheid et al. 1994 for details) and is used to calculate the formal valence of the element of interest dissolved in the silicate melt. Fit coefficients resulting from linear regressions of oxygen fugacity dependences of D_{sol}(M/S) for Ni, Co, Fe, Mo, and W and calculated formal valences are given in Table 4a. Nickel, Co, and Fe are dissolved as divalent cations and W as W^{4+}-cations in the silicate liquids. The least square regression of Mo-D_{sol}(M/S) versus log fO_2 changes its slope at an oxygen fugacity about one log-unit below the iron-wüstite buffer (IW-1) indicating dissolution of Mo^{6+}-cations under oxidizing conditions and Mo^{4+}-cations under more reduced conditions.

Molybdenum and W partition coefficients derived from solubilities in FeO-containing systems (unpublished data and Millbillillie) at oxygen fugacities above IW-1 are in good agreement with Mo- and W-D_{sol}(M/S) in FeO-free systems (Holzheid et al. 1994; Ertel et al. 1996), while Mo- and W-D_{sol}(M/S) in FeO-containing systems (Millbillillie) at more reducing conditions (experiment Mill-11; log fO_2 = –12.6) deviate from those in FeO-free systems. The disagreement between D_{sol}(M/S) values in Millbillillie experiments and in FeO-free experiments is more pronounced for Mo than for W, as the overall scatter of W-D_{sol}(M/S) values is larger. Since Mo, W, and FeNiCo samples were simultaneously in the furnace in experiment Mill-11 and Fe-, Ni-, and Co-D_{sol}(M/S) values of Mill-11 agree well with all other Fe-, Ni-, and Co-D_{sol}(M/S) values, run condition can be assumed to be as specified. The reason for the deviation of Mo and W is unclear, but might be related to activity coefficients of Mo and W in binary FeMo and FeW alloys that are lower than the appropriate values. Alternatively, the activity coefficients of Mo and W oxides may depend on the composition of the silicate melt. At elevated pressures, Walter and Thibault (1995) and Jana and Walker (1997) were able to correlate changes in the solubility behavior of MoO_3 and WO_3 with the Si/Mg ratio of the silicate melt and the degree of polymerization of the silicate melt. These findings might not be easily applicable to our study. Within the oxygen fugacity range covered by our experiments, the dissolved Mo cations change their valence state from Mo^{6+} to Mo^{4+} at an oxygen fugacity of about IW-1, while W is dissolved as W^{4+} cation in the silicate liquid within the entire oxygen fugacity range. O'Neill and Eggins (2002) report variations in activity coefficients of Mo oxides that are more pronounced for MoO_2 species than for MoO_3 species in the silicate melt at one atmosphere total pressure. The dominant Mo oxide species in experiment Mill-11 is MoO_2. The change in activity coefficients of Mo oxides as function of the silicate liquid postulated by O'Neill and Eggins (2002) might cause the observed deviation of Mo-D_{sol}(M/S), the deviation of W-D_{sol}(M/S) remains unexplained. However, the least square regressions (Fig. 2; Table 4a) do not include the Mo- and W-D_{sol}(M/S) values at $10^{-12.6}$ (experiment Mill-11).

The temperature dependences of Ni, Co, and Fe solubilities were investigated by additional experiments over a temperature range from 1211 to 1600 °C (experiments Mill-2, 6, 8, 9, 12, and 14) (Table 2). Oxygen fugacities in these experiments were within an oxygen fugacity range of 1.04 ± 0.05 log units below the Fe-FeO buffer. Nickel-, Co-, and Fe-D_{sol}(M/S) are recalculated to IW-1 using the oxygen fugacity dependence of Fig. 1 to exclude any change in D_{sol}(M/S) that is due to variations in oxygen fugacity and not in temperature. These recalculated Ni-, Co-, and Fe-D_{sol}(M/S) are plotted as function of temperature in Fig. 3. Best-fit lines (solid lines) are based on all experimental data. Fit

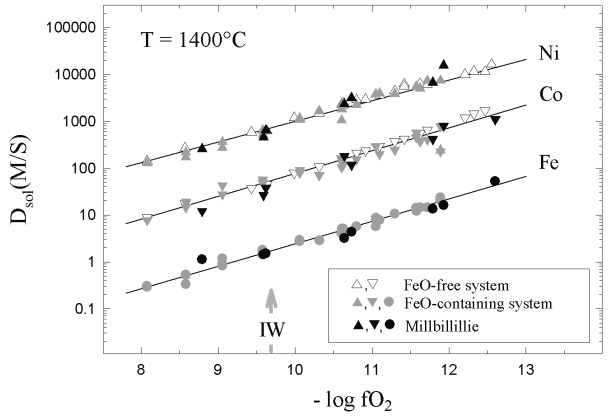

Fig. 1. Solubility metal-silicate partition coefficients D_{sol}(M/S) of Ni, Co, and Fe as function of oxygen fugacity at isothermal conditions (1400 °C). Partition coefficients with Millbillillie as silicate starting material are plotted as closed symbols. Partition coefficients obtained in earlier studies are plotted as open symbols (FeO-free system; Holzheid et al. 1994) and gray symbols (FeO-containing system; Holzheid and Palme 1996). Least square regressions (solid lines) are based on all experimental data. Formal valences of the dissolved metal cations are 2+ for Ni, Co, and Fe.

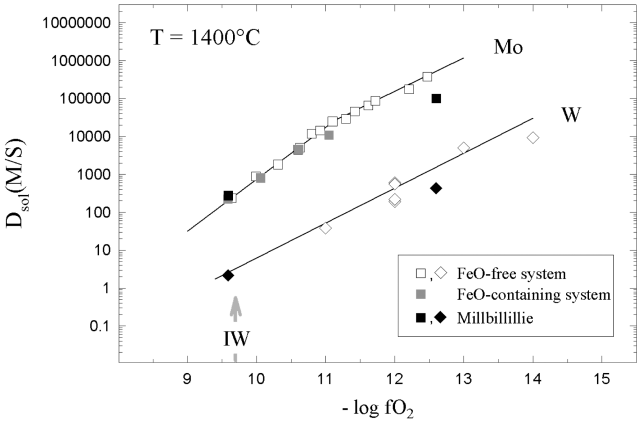

Fig. 2. Solubility metal-silicate partition coefficients D_{sol}(M/S) of Mo and W as function of oxygen fugacity at isothermal conditions (1400 °C). Partition coefficients with Millbillillie as silicate starting material are plotted as closed symbols. Partition coefficients obtained in earlier studies (Holzheid et al. 1994; Holzheid and Palme 1996) are plotted as open symbols (FeO-free system; Mo: Holzheid et al. 1994; W: Ertel et al. 1996) and gray symbols (FeO-containing system; Mo: unpublished data). Least square regressions (solid lines) are based on all experimental data with the exception for Mo- and W-D_{sol}(M/S) values at $10^{-12.6}$ (see text for more detail). Formal valence of the dissolved W cations is 4+. Molybdenum seems to change its dominant formal valence state from Mo^{6+} cations under oxidizing conditions and Mo^{4+}-cations under more reduced conditions.

coefficients resulting from linear regressions of temperature dependences of D_{sol}(M/S) for all elements investigated are given in Table 4b. Partition coefficients of Ni and Co show a slight decrease with increasing temperature. The temperature dependence is more pronounced for Ni than for Co. As expected, Fe partition coefficients show no temperature dependence along IW-1. The temperature dependence of Ni- and Co-D_{sol}(M/S) is independent of the chemical composition of the silicate melt. The slope of the temperature dependence of Mo- and W-D_{sol}(M/S) overlap within the uncertainties (Table 4b).

APPLICATION OF THE METAL-SILICATE PARTITION COEFFICIENTS TO MODELS OF CORE FORMATION IN THE EPB AND PETROGENESIS OF EUCRITIC METEORITES

Various hypotheses attempt to model the early history of the EPB, or the HED parent body, respectively, and the siderophile element abundances in the HED meteorites. Two hypotheses can be considered as "endmember models:" one of the end-member models explains main group and Stannern trend eucrites as the result of relatively low degrees of equilibrium (batch) partial melting of a chondritic source, first suggested by Stolper (1975). The counterpart model explains all HED meteorites as results of various stages of fractional crystallization processes in an extensively or completely molten EPB, first suggested by Mason (1962). Modified models that combine aspects of both endmember models are described by Hewins and Newsom (1988) and Righter and Drake (1996, 1997). A brief compilation of the various hypotheses is given in Drake (2001) and in Mittlefehldt and Lindstrom (2003).

In the following the two endmember models will be described in more detail, and metal-silicate partition behavior of the siderophile elements Ni, Co, W, Mo, and also Fe (experimentally determined in this study) will be used for evaluation of the models.

Equilibrium Between Metal and Silicate Phases at Low Degrees of Partial Melting

The model was first suggested by Stolper (1975), modified by, e.g., Stolper (1977) and Consolmagno and Drake (1977), and revisited by Jurewicz et al. (1993). The compositional variation of eucritic meteorites is explained as a result of melting processes with variable degrees (4–30%) of equilibrium (batch) partial melting of a metal-bearing, chondritic source region, representing the EPB, at low pressure and temperatures followed by fractional crystallization and crystal accumulation. Stolper (1977) explicitly proposed that the siderophile element abundances in main group and Stannern trend eucrites are the result of equilibration of partial melts with metal in the source of the eucrites at temperatures of about 1190 °C. Diogenites are regarded as cumulates of phases separated from more advanced partial melts of the same source. Howardites are polymict breccias containing fragments sampling the spectrum of differentiated liquids and cumulates developed

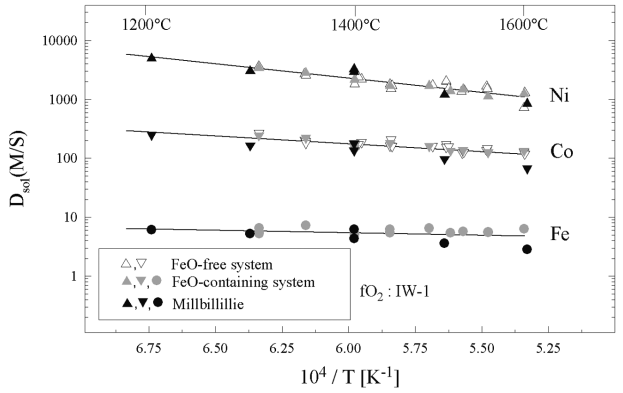

Fig. 3. Metal-silicate partition coefficients D_{sol}(M/S) of Ni, Co, and Fe as function of temperature at an oxygen fugacity of one log-unit below the iron-wüstite (IW) buffer. Partition coefficients with Millbillillie as silicate starting material are plotted as full symbols. Partition coefficients obtained in earlier studies are plotted as open symbols (FeO-free system; Holzheid et al. 1994) and gray symbols (FeO-containing system; Holzheid and Palme 1996). Least square regressions (solid lines) are based on all experimental data. The temperature dependence is more pronounced for Ni than for Co.

from the range of primary magmas produced by variable degrees of partial melting of the source.

Based on the FeO contents in eucritic meteorites (Table 1) and the Fe content in H-chondrite metal representing the EPB-core composition (Table 5), an oxygen fugacity of about IW-1 is calculated for the metal-silicate equilibrium that prevailed during source metal-eucritic melt equilibrium. Applying the metal-silicate partition coefficients obtained in this study to the expected siderophile element contents in eucrites leads to the results given in Table 6a. Uncertainties in extrapolating experimentally determined metal-silicate partition coefficients to appropriate oxygen fugacities and a temperature of 1190 °C are taken into account. Concentrations of Fe, Ni, Co, W, and Mo in eucritic melts, labelled as silicate in Table 6a, are calculated for three different metal fractions of H-chondritic composition and eucritic silicate. Equilibrium between silicate melt and solid silicate phases was neglected, as only siderophile elements were considered. The observed Co content in Millbillillie reflects equilibrium distribution of an eucritic melt with 25% metal in the source. But the observed Ni content in Millbillillie is lower by more than a factor of 2 compared to the expected amount from equilibrium distribution at the same identical metal fraction and oxygen fugacity. Moreover, the observed W and Mo concentrations in Millbillillie are higher by a factor of 3 and 30, respectively, compared to the calculated W and Mo contents. We wish to reiterate that the partition coefficients employed for these calculations were obtained in experiments with eucritic melts as starting material and should therefore provide an excellent basis to evaluate the "partial melting" model. That the post-run silicate charges deviate slightly from the starting silicate is not

Table 5. Composition of H-chondrite metal.

Fe (wt%)	Ni (wt%)	Co (ppm)	W (ppm)	Mo (ppm)
89.3	9.05	4670	0.778	4.18

Concentrations taken from Kong and Ebihara 1997 (Table 1, mean H4–6).

relevant, as the effect of the silicate melt composition on the Ni-D_{sol}(M/S) can be neglected. It thus appears that equilibrium partial melting of an H-chondrite source is inadequate for explaining the origin of eucritic melts. Palme and Rammensee (1981) have provided an additional argument against a simple partial melting model for eucrites. In many basaltic meteorites and lunar basalts, moderately siderophile elements such as W but also Mo are positively correlated with refractory lithophile incompatible elements such as La, Ta, or Ce (e.g., Palme and Rammensee 1981; Righter and Drake 1997). This positive correlation is indicative of incompatible behavior of the lithophile incompatible elements (La, Ta) and the siderophile incompatible element (W). Incompatible behavior of W is only possible if metal is absent in the source region of eucrites; otherwise W contents would be buffered by the metal. The observed incompatible behavior of W therefore contradicts the partial melting hypothesis with chondritic metal in the source.

Why was Stolper (1977) able to propose that the siderophile element abundances in eucrites are the result of equilibration between metal and silicate phases at low degrees of partial melting? The partition coefficients available to Stolper (1977) were incorrect. More recent studies (see, e.g., Walter et al. 2000 for literature compilation until 1999; this study) have shown that the metal-silicate partition coefficients used by Stolper (1977) are not appropriate to the oxygen fugacity that prevailed during source metal-eucritic melt equilibrium. These metal-silicate partition coefficients, estimated by Hewins and Goldstein (1974), range from 6000 to 8000 for Ni and about 1000 for Co. Taking our experimentally derived dependences of D_{sol}(M/S) of Ni and Co on oxygen fugacity (Fig. 1; assuming dissolution of NiO and CoO in silicate liquids) and on temperature (Fig. 3), one can calculate the oxygen fugacities that are required to match the metal-silicate partition coefficients of Hewins and Goldstein (1974). At a temperature of 1190 °C, the required oxygen fugacities are IW-1.02 (Ni D_{sol}[M/S] = 6000), IW-1.27 (Ni D_{sol}[M/S] = 8000), and IW-2.06 (Co D_{sol}[M/S] = 1000). As the oxygen fugacity values range within more than one log unit and are, at least for Co, significantly more reducing than IW-1, the use of the metal-silicate partition coefficients of Hewins and Goldstein (1974) by Stolper (1977) has to be examined with the knowledge gained in the 30 years since these publications. Neither do the Ni and Co D_{sol}(M/S) values reflect a single oxygen fugacity nor have the oxygen fugacities the appropriate values, that are required to explain the FeO contents in eucritic meteorites by source metal- eucritic melt equilibrium distribution.

Table 6a. Calculations of silicate compositions as results of partial melting and fractional crystallization sequences.

Partial melting					T = 1190 °C	
fO_2 (Δ IW)	Metal fraction (%)	Silicate Fe (wt%)	Ni (ppm)	Co (ppm)	W (ppb)	Mo (ppb)
–0.94	18	15 ± 2.2	13 ± 1.6	10 ± 1.7	12 ± 5.9	0.53 ± 0.15
–0.99	33	15 ± 2.2	6.7 ± 0.82	4.8 ± 0.82	11 ± 5.4	0.48 ± 0.14
–0.97	25	15 ± 2.2	8.8 ± 1.1	6.5 ± 1.1	11 ± 5.4	0.50 ± 0.14
Eucrite analyses[a]		15	<3.5	6.4	31	15

Table 6b. Calculations of silicate compositions as results of partial melting and fractional crystallization sequences.

Metal-silicate equilibrium followed by fractional crystallization					T = 1600 °C	
Results of global metal-silicate equilibrium						
fO_2 (ΔIW)	Metal fraction (%)	Silicate Fe (wt%)	Ni (ppm)	Co (ppm)	W (ppb)	Mo (ppb)
–1.44	22	12 ± 1.7	33 ± 4.0	13 ± 2.2	19 ± 9.3	1.1 ± 0.31
–1.43	19	12 ± 1.7	38 ± 4.7	15 ± 2.6	20 ± 9.8	1.1 ± 0.31
BS-EPB[b]		12	38	13	14	6.6
Results of fractional crystallization based on the silicate composition at ΔIW-1.43 (fO_2) and 19% (metal fraction)						
Fraction of remaining liquid	Silicate Fe (wt%)	Ni (ppm)	Co (ppm)	W (ppb)	Mo (ppb)	
F = 0.43[c]	12–14[d]	0.2–3.0[d, e]	6.4[d, e]	42–44[d]	2.2–2.4[f]	
F = 0.75[g]	13–17[h]	0.2–3.4[h–j]	5.5–7.0[h]	51–54[k]	1.6–3.2[f, l]	
Eucrite analyses[a]	15	<3.5	6.4	31	15	

[a]Fe, Ni, Co concentrations taken from Table 1 (Millbillillie); W and Mo concentrations from Juvinas (W: Palme and Rammensee 1981; Mo: Newsom and Palme 1984).
[b]Calculated bulk silicate (BS) composition of the eucrite parent body (EPB) taken from Dreibus and Wänke (1980), except for Mo. The Mo content is calculated by applying the constant Mo/W ratio of about 0.5 in eucrites (Newsom 1985).
[c]Fraction of remaining liquid; (1-F) = fraction of crystallized olivine.
[d]Element content in melt based on calculation using $D_{(ol/melt)}$ values of Gaetani and Grove (1997).
[e]Element content in melt using $D^{(ol/melt)}$ values of Seifert et al. (1988).
[f]Element content in melt using $D^{(ol/melt)}$ values of Dunn and Sen (1994).
[g]Fraction of remaining liquid; (1-F) = fraction of crystallized orthopyroxene.
[h]Element content in melt using $D^{(opx/melt)}$ values of Kennedy et al. (1993).
[i]Element content in melt using $D^{(opx/melt)}$ values of Mysen (1976).
[j]Element content in melt using $D^{(opx/melt)}$ values of Mysen (1978).
[k]Element content in melt using $D^{(opx/melt)}$ values of Luhr et al. (1984).
[l]Element content in melt using $D^{(opx/melt)}$ values of Walker et al. (1992).

Equilibrium Between Metal and Silicate Phases During Extensive Melting Followed by Fractional Crystallization

The model was first suggested by Mason (1962), modified by, e.g., McCarthy et al. (1973), Ikeda and Takeda (1985), Warren (1985), Warren and Jerde (1987), Bartels and Grove (1991), and Grove and Bartels (1992), and revisited by Ruzicka et al. (1997a, 1997b).

The model explains the main group noncumulate eucrites as residual melts in a magma with the major element composition of the HED parent asteroid undergoing simple fractional crystallization at higher temperatures and pressures, while diogenites represent earlier crystallized cumulates in the same magmatic system.

We will again use our experimentally determined partition coefficients of Fe, Ni, Co, W, and Mo between coexisting metal and silicate phases to evaluate the model of metal-silicate equilibrium to explain the contents of Fe, Ni, Co, W, and Mo in the bulk silicate of the EPB followed by fractional crystallization primary of olivine and subsequent of orthopyroxene to model the compositions of eucritic meteorites. In Table 6b, expected concentrations of Fe, Ni, Co, W, and Mo in the bulk silicate portion of the eucrite parent body (BS-EPB), labelled as silicate in Table 6b, are calculated for two metal fractions at a temperature of 1600 °C, i.e., a temperature at which coexistence of silicate liquid and metal liquid phases is assured. Oxygen fugacities (first column in Table 6b) are chosen in such a way that the expected FeO content in the BS-EPB will match the FeO content of the BS-EPB as estimated by Dreibus and Wänke (1980), assuming equilibrium between BS-EPB and the metal portion of the parent body. Calculated Ni, Co, and W abundances based on our new partition coefficients agree within uncertainties with the estimated abundances in the bulk silicates of the eucrite parent body. This is not too surprising since Dreibus and Wänke (1980) have based their estimates on existing metal-silicate partition coefficients. The more important result is that Mo abundances do not fit at all with the abundances predicted by Dreibus and Wänke (1980). Additional extraction of the chalcophile element Mo

Table 7. Comparison of W and Mo absolute and relative abundances in silicate mantles of planetary bodies.

Silicate portion	W (ppb)	Mo (ppb)	(W/Mo)	$(W/Mo)_{CI}$[a]
Moon[b]	18	2.2	8.2	82
EPB[c]	14	6.6	2.1	21
Mars[d]	105	118	0.89	8.9
Earth (PM)[e]	16	45	0.35	3.5

[a]CI-normalized W/Mo ratios; W and Mo abundances in CI meteorites from Palme and Jones (2003).
[b]W: Wänke and Dreibus (1986), Mo: Newsom (1986). See also O'Neill (1991).
[c]Dreibus and Wänke (1980).
[d]Dreibus and Wänke (1988).
[e]PM = primitive mantle; O'Neill and Palme (1998).

from silicate melts with a sulfur-bearing metallic liquid would even lower the calculated Mo abundances. The calculated BS-EPB composition, based on an oxygen fugacity 1.43 log units more reducing than the IW-buffer and at a metal fraction of 19%, was used as starting silicate composition to compute the element concentration in the residual silicate, i.e., the parental liquid of eucritic meteorites, as result of fractional crystallization of olivine followed by orthopyroxene after equilibration of metal and silicate phases. The olivine-orthopyroxene reaction boundary moves away from the SiO_2 corner of the olivine-plagioclase-quartz pseudoternary system at low pressures (see Fig. 2 in Bartels and Grove 1991 and Fig. 1 in Grove and Bartels 1992). Based on the pressure effect on the olivine-orthopyroxene cotectic, Grove and Bartels (1992) postulated fractional crystallization at higher pressures (i.e., in the interior of the EPB) as prerequisite to be able to relate diogenites with eucrites by fractional crystallization. In accordance with Righter and Drake (1997), we used olivine/melt partition coefficients at elevated pressures, if available in the literature, in order to account for the pressure effect mentioned above. Olivine/melt partition coefficient values, $D^{ol/melt}$, of Fe, Ni, Co, and W, reported in Seifert et al. (1988) and Gaetani and Grove (1997), covering a pressure range from 1 atm to 3.5 GPa, and 1 atm $D^{ol/melt}$ values of Mo, reported in Dunn and Sen (1994), were used for these calculations. The fraction of remaining liquid was defined in such a way that the calculated Co concentration in the residual silicate liquid matches the observed Co content in the eucrite Millbillillie (Table 1). Concentrations of Fe, Ni, W, and Mo were then generated using the defined fraction of remaining liquid and the $D^{ol/melt}$ values available in the literature. The range in the calculated concentrations of Fe, Ni, W, and Mo in the residual liquid in Table 6b reflects variations in the literature $D^{ol/melt}$ values. Fractional crystallization of olivine will lower the Ni concentration and increase the W and Mo concentrations in the residual silicate liquid. As $D^{ol/melt}$ values of Fe are close to unity, the change in Fe content during fractional crystallization of olivine is small. To compute the changes in composition of the residual liquid during crystallization of orthopyroxene, orthopyroxene/melt partition coefficient values ($D^{opx/melt}$) from the literature were used ($D^{opx/melt}$ of Fe: Kennedy et al. 1993 [at 1 atm pressure]; $D^{opx/melt}$ of Ni: Mysen 1976, Mysen 1978, Kennedy et al. 1993 [1 atm – 2 GPa]; $D^{opx/melt}$ of Co: Kennedy et al. 1993 [1 atm]; $D^{opx/melt}$ of W: Luhr et al. 1984 [0.4 GPa]; $D^{opx/melt}$ of Mo: Walker et al. 1992, Dunn and Sen 1994 [1 atm–5.5 GPa]). This time the fraction of remaining liquid was defined in such a way that the calculated Fe concentration in the residual silicate liquid matches the observed Fe content in the eucrite Millbillillie (Table 1). In analogy to the modeling of the fractional crystallization of olivine, concentrations of Ni, Co, W, and Mo in the residual silicate liquid were calculated using the defined fraction of remaining liquid and the literature $D^{opx/melt}$ values. The range in the calculated concentrations of Fe, Ni, Co, W, and Mo in the residual liquid in Table 6b reflects again variations in the literature $D^{opx/melt}$ values. Although the observed Fe and Co concentrations in eucrites are bracketed by the calculated values and only upper limits of Ni in the eucrites are known, Fe, Ni, and Co concentration levels in eucrites seem to be able to be explained by equilibrium distribution between metal and silicate phases during extensive melting followed by fractional crystallization of olivine and orthopyroxene. Expected concentrations of W and Mo in the residual liquid are higher by a factor of about 1.7 (W) and lower by a factor of about 6.3 (Mo) when compared to observed W and Mo contents in eucrites. Molybdenum is more siderophile and more chalcophile than W. Sulfide-silicate partition coefficients of Mo are two to three orders of magnitude larger compared to W (e.g., Lodders and Palme 1991 and references therein). Molybdenum would be therefore preferentially extracted into sulfur-bearing phases at any time of the fractional crystallization sequence. Sulfur abundances in eucrites range from about 400 to 9700 ppm (e.g., Gibson and Moore 1983; Palme et al. 1983; Hartmetz et al. 1989) with the accessory mineral troilite as the dominant sulfur-bearing phase. No correlation between the eucritic compositional types and the sulfur abundances seems to exist (Gibson and Moore 1983). The Mo concentration, listed in Table 6, is taken from Juvinas (Newsom and Palme 1984). Sulfur abundances in Juvinas range from 1140 ± 30 to 2550 ± 70 ppm (Gibson and Moore 1983). These sulfur abundances are close to or even higher than sulfur solubility limits in silicate liquids (Holzheid and Grove 2002; Mavrogenes and O'Neill 1999). It might be therefore possible that the majority of the Mo in Juvinas is concentrated in separate troilite phases that formed due to sulfur oversaturation of the residual liquid. The observed high Mo concentrations in eucrites would than not reflect any mineral/melt partition distribution. The high Mo concentrations would rather be related to local Mo enrichments in eucrites, as they are most likely concentrated in the separate sulfide phase troilite.

Mason (1962) and the other studies listed above had focused solely on data for major elements and highly and moderately incompatible lithophile trace elements. Siderophile and/or chalcophile trace element concentrations in eucrites were not included in their calculations of the liquid lines of descent. By only focusing on data for siderophile and/or chalcophile elements, we and they are able to propose that eucrites represent residual liquids of a magma that undergoes fractional crystallization of olivine and orthopyroxene.

CONCENTRATIONS OF W AND MO IN SILICATE MANTLES OF PLANETARY BODIES

The new data on metal-silicate partitioning of Ni, Co, W, and Mo are more precise than earlier data as we used eucritic melts as silicate liquids, minimizing the effect of silicate melt composition on the partition coefficients. The results clearly show that siderophile element abundances in eucritic meteorites cannot be explained by partial melting of an H-chondritic metal-containing source, as shown by comparison of observed siderophile element concentrations in eucritic meteorites with element abundances calculated using metal-silicate partition coefficients. Fractional crystallization of the eucritic basalts after metal-silicate equilibrium during extensive melting can better explain the siderophile element concentrations in eucritic meteorites. However, the discrepancies between observed and calculated Mo abundances in eucritic meteorites and BS-EPB remain unsolved. One explanation is that the Mo content in eucrites does not reflect mineral/melt partition distribution. The high Mo concentrations in eucrites would then be the result of local Mo enrichments in separate sulfide phases (see above for more details).

Another explanation of the discrepancy is based on a metal-silicate partition distribution. Absolute W and Mo concentrations, W/Mo ratios, and CI-normalized W/Mo ratios in the silicate portions of Moon, EPB, Mars, and the primitive mantle of the Earth are listed in Table 7. All W/Mo ratios are larger than the CI-W/Mo ratio of 0.1 (Palme and Jones 2003), indicating the stronger extraction of Mo relative to W into metallic phases. If the abundances of W and Mo in the silicate portion of the planetary bodies reflect equilibrium partitioning of both elements between metal and silicate phases at ambient pressure, the ratios should be identical to the experimentally derived W/Mo partition ratio of 331 at 1 atm and 1400 °C (this work). This is obviously not the case. The W/Mo ratios are significantly smaller. Tungsten metal-silicate partition coefficients decrease with increasing pressure. Molybdenum metal-silicate partition coefficients increase with increasing pressure (Walter et al. 2000). The W/Mo partition ratio therefore decreases with increasing pressure. The decrease in the W/Mo partition ratio should be more pronounced for larger bodies (i.e., Earth) than for smaller bodies (i.e., EPB or the Moon). Based on the size of the planetary bodies, the pressure dependence of the W and Mo partition coefficients can be neglected for both EPB and the Moon. It is unclear if the large difference in the W/Mo ratio between the Moon and EPB is real. There is definitely a need for more analytical data on Mo in eucrites, as all reported analytical data are from a single source. However, the smaller CI-normalized W/Mo ratios of Mars and Earth compared to these of the Moon and EPB (Table 7) might directly reflect the postulated W/Mo pressure dependence. New partition data on Mo indeed indicate a fairly strong pressure effect (Agee and Martin 2007). In order to strengthen this observation, it is desirable to know more precisely the partition behavior of W and Mo over an extended range of pressures.

Acknowledgments–The experiments were carried out at Universität zu Köln in Cologne. Experimental samples and aliquots of eucritic meteorites were irradiated at the TRIGA-reactor of the Institut für Anorganische Chemie und Kernchemie der Universität Mainz. We thank the staff of the reactor for their help. Thorough reviews by T. L. Grove and D. W. Mittlefehldt and comments by the associate editor, K. Righter, led to significant improvement of this paper. This research was supported in part by the German Science Foundation (DFG).

Editorial Handling—Dr. Kevin Righter

REFERENCES

Agee C. B. and Martin E. 2007. Molybdenum solubility in silicate melt at high pressures and temperatures: Experimental constraints on planetary core formation (abstract #2170). 38th Lunar and Planetary Science Conference. CD-ROM.

Barrat J. A., Blichert-Toft J., Gillet Ph., and Keller F. 2000. The differentiation of eucrites: The role of in situ crystallization. *Meteoritics & Planetary Science* 35:1087–1100.

Bartels K. S. and Grove T. L. 1991. High-pressure experiments on magnesian eucrite compositions: Constraints on magmatic processes in the eucrite parent body. Proceedings, 21st Lunar and Planetary Science Conference. pp. 351–365.

Basaltic Volcanism Study Project (BVSP). 1981. *Basaltic volcanism on the terrestrial planets*. New York: Pergamon Press. 1286 p.

Binzel R. P. and Xu S. 1993. Chips off of asteroid 4 Vesta: Evidence for the parent body of basaltic achondrite meteorites. *Science* 260:186–191.

Borisov A., Palme H., and Spettel B. 1994. Solubility of palladium in silicate melts: Implications for core formation in the Earth. *Geochimica et Cosmochimica Acta* 58:705–716.

Clayton R. N. and Mayeda T. K. 1996. Oxygen isotopes studies of achondrites. *Geochimica et Cosmochimica Acta* 60:1999–2017.

Consolmagno G. J. and Drake M. J. 1977. Composition and evolution of the eucrite parent body: Evidence from rare earth elements. *Geochimica et Cosmochimica Acta* 41:1271–1282.

Drake M. J. 2001. The eucrite/Vesta story. *Meteoritics & Planetary Science* 36:501–513.

Dreibus G. and Wänke H. 1980. The bulk composition of the eucrite

parent asteroid and its bearing on planetary evolution. *Zeitschrift für Naturforschung* 35a:204–216.

Dreibus G. and Wänke H. 1988. Chemistry and physics of the Martian interior derived from SNC meteorites (abstract). *Chemical Geology* 70:7.

Dunn T. and Sen C. 1994. Mineral/matrix partition coefficients for orthopyroxene, plagioclase, and olivine in basaltic to andesitic systems—A combined analytical and experimental study. *Geochimica et Cosmochimica Acta* 58:717–733.

Ertel W., O'Neill H. St. C., Dingwell D. B., and Spettel B. 1996. Solubility of tungsten in a haplobasaltic melt as function of temperature and oxygen fugacity. *Geochimica et Cosmochimica Acta* 60:1171–1180.

Gaetani G. A. and Grove T. L. 1997. Partitioning of moderately siderophile elements among olivine, silicate melt, and sulfide melt: Constraints on core formation in the Earth and Mars. *Geochimica et Cosmochimica Acta* 61:1829–1846.

Gibson E. K. and Moore C. B. 1983. Sulfur in achondritic meteorites (abstract). Proceedings, 14th Lunar and Planetary Science Conference. pp. 247–248.

Grove T. L. and Bartels K. S. 1992. The relation between diogenite cumulates and eucrite magmas. 22nd Lunar and Planetary Science Conference. pp. 437–445.

Guillermet A. F. 1989. Assessing the thermodynamics of the Fe-Co-Ni system using a calphad predictive technique. *Calphad* 13:1–22.

Hartmetz C. P., Gibson E. K., and Socki R. A. 1989. Total carbon and sulfur abundances in Antarctic carbonaceous chondrites, ordinary chondrites, and eucrites (abstract). *Meteoritics* 24:274.

Hewins R. H. and Goldstein J. I. 1974. Metal-olivine associations and Ni-Co contents in two Apollo 12 mare basalts. *Earth and Planetary Science Letters* 24:59–70.

Hewins R. H. and Newsom H. E. 1988. Igneous activity in the early solar system. In *Meteorites and the early solar system*, edited by Kerridge J. F. and Matthews M. S. Tucson, Arizona: The University of Arizona Press. pp. 73–101.

Holzheid A. and Palme H. 1996. The influence of FeO on the solubility of Co and Ni in silicate melts. *Geochimica et Cosmochimica Acta* 60:1181–1193.

Holzheid A. and Grove T. L. 2002. Sulfide saturation limits in silicate melts and their implications to core formation scenarios for terrestrial planets. *American Mineralogist* 87:227–237.

Holzheid A., Borisov A., and Palme H. 1994. The effect of oxygen fugacity and temperature on solubilities of nickel, cobalt, and molybdenum in silicate melts. *Geochimica et Cosmochimica Acta* 58:1975–1981.

Ichise E., Maruo T., Sasho H., Ueshima Y., and Mori T. 1980. Knudsen cell-mass spectrometric determination of activities in Fe-Mo alloys. *Tetsu to Hagane* 66:1075–1083.

Ikeda Y. and Takeda H. 1985. A model for the origin of basaltic achondrites based on the Yamato-7308 howardite. *Journal of Geophysical Research* 90:C649–C663.

Jana D. and Walker D. 1997. The influence of silicate melt composition on distribution of siderophile elements among metal and silicate liquids. *Earth and Planetary Science Letters* 150: 463–472.

Jurewicz A. J. G., Mittlefehldt D. W., and Jones J. H. 1993. Experimental partial melting of Allende (CV) and Murchison (CM) chondrites and the origin of asteroidal basalts. *Geochimica et Cosmochimica Acta* 57:2123–2139.

Kennedy A. K., Lofgren G. E., and Wasserburg G. J. 1993. An experimental study of trace element partitioning between olivine, orthopyroxene, and melt in chondrules—Equilibrium values and kinetic effects. *Earth and Planetary Science Letters* 115:177–195.

Kitts K. and Lodders K. 1998. Survey and evaluation of eucrite bulk compositions. *Meteoritics & Planetary Science* 33:A197–A213.

Kong P. and Ebihara M. 1997. The origin and nebular history of the metal phase of ordinary chondrites. *Geochimica et Cosmochimica Acta* 61:2317–2329.

Lodders K. and Palme H. 1991. On the chalcophile character of molybdenum: Determination of sulfide/silicate partition coefficients of Mo and W. *Earth and Planetary Science Letters* 103:311–324.

Luhr J. F., Carmichael I. S. E., and Varekamp J. C. 1984. The 1982 eruptions of El Chichon volcano, Chiapas, Mexico: Mineralogy and petrology of the anhydrite-bearing pumices. *Journal of Volcanology and Geothermal Research* 23:69–108.

Mason B. 1962. *Meteorites.* New York: John Wiley and Sons. 273 p.

Mavrogenes J. A. and O'Neill H. St. C. 1999. The relative effects of pressure, temperature, and oxygen fugacity on the solubility of sulfide in mafic magmas. *Geochimica et Cosmochimica Acta* 63: 1173–1180.

McCarthy T. S., Erlank A. J., and Willis J. P. 1973. On the origin of eucrites and diogenites. *Earth and Planetary Science Letters* 18: 433–442.

McCord T. B., Adams J. B., and Johnson T. V. 1970. Asteroid Vesta: Spectral reflectivity and compositional implications. *Science* 168:1445–1447.

Mittlefehldt D. W. and Lindstrom M. M. 2003. Geochemistry of eucrites: Genesis of basaltic eucrites, and Hf and Ta as petrogenetic indicators for altered Antarctic eucrites. *Geochimica et Cosmochimica Acta* 67:1911–1935.

Mysen B. 1976. Partitioning of samarium and nickel between olivine, orthopyroxene, and liquid: Preliminary data at 20 kbar and 1025 °C. *Earth and Planetary Science Letters* 31:1–7.

Mysen B. 1978. Experimental determination of nickel partition coefficients between liquid, pargasite, and garnet peridotite minerals and concentration limits of behavior according to Henry's Law at high pressure and temperature. *American Journal of Science* 278:217–243.

Newsom H. E. 1985. Molybdenum in eucrites: Evidence for a metal core in the eucrite parent body. *Journal of Geophysical Research* 90:C613–C617.

Newsom H. E. and Palme H. 1984. The determination of molybdenum in geological samples by neutron activation analysis. *Journal of Radioanalytical Nuclear Chemistry* 87:273–282.

Newsom H. E. 1986. Constraints on the origin of the Moon from the abundance of molybdenum and other siderophile elements. In *Origin of the Moon*, edited by Hartmann W. K., Phillips R. J., and Taylor G. J. Houston: Lunar and Planetary Institute. pp. 203–229.

O'Neill H. St. C. 1991. The origin of the Moon and the early history of the Earth—A chemical model. Part I: The Moon. *Geochimica et Cosmochimica Acta* 55:1135–1157.

O'Neill H. St. C. and Palme H. 1998. Composition of the silicate Earth: Implications for accretion and core formation. In *The Earth's mantle: Composition, structure, and evolution*, edited by Jackson I. Cambridge: Cambridge University Press. pp. 3–126.

O'Neill H. St. C. and Eggins S. M. 2002. The effect of melt composition on trace element partitioning: An experimental investigation of the activity coefficients of FeO, NiO, CoO, MoO_2, and MoO_3 in silicate melts. *Chemical Geology* 186:151–181.

Palme H. and Rammensee W. 1982. The significance of W in planetary differentiation processes: Evidence from new data on eucrites. Proceedings, 12th Lunar and Planetary Science Conference. pp. 949–964.

Palme H., Spettel B., Burghele A., Weckwerth G., Wänke H.,

Delaney J. S., and Prinz H. 1983. Elephant Moraine polymict eucrites: A eucrite-howardite compositional link (abstract). 14th Lunar and Planetary Science Conference. pp. 590–591.

Palme H. and Jones A. 2003 Solar system abundances of the elements. In *Meteorites, comets, and asteroids*, edited by Davis A. H. Treatise on Geochemistry, vol. 1, edited by Holland H. D. and Turekian K. K. Oxford: Elsevier-Pergamon. pp. 41–62.

Righter K. and Drake M. J. 1996. Core formation in Earth's Moon, Mars, and Vesta. *Icarus* 124:513–529.

Righter K. and Drake M. J. 1997. A magma ocean on Vesta: Core formation and petrogenesis of eucrites and diogenites. *Meteoritics & Planetary Science* 32:929–944.

Ruzicka A., Snyder G. A., and Taylor L. A. 1997a. Formation of eucrites and diogenites in a magma ocean on the HED parent body (abstract #1426). 28th Lunar and Planetary Science Conference. CD-ROM.

Ruzicka A., Snyder G. A., and Taylor L. A. 1997b. Could eucrites have formed as residual liquids in a magma ocean (abstract #1434)? 28th Lunar and Planetary Science Conference. CD-ROM.

Seifert S., O'Neill H. St. C., and Brey G. 1988. The partitioning of Fe, Ni, and Co between olivine, metal, and basaltic liquid—An experimental and thermodynamic investigation, with application to the composition of the lunar core. *Geochimica et Cosmochimica Acta* 52:603–616.

Stolper E. M. 1975. Petrogenesis of eucrite, howardite, and diogenite meteorites. *Nature* 258:220–222.

Stolper E. M. 1977. Experimental petrology of eucritic meteorites. *Geochimica et Cosmochimica Acta* 41:587–611.

Takeda H., Miyamoto M., Ighi T., and Reid A. M. 1976. Characterization history of a crust of their parent body. *Journal of Geophysical Research* 90:C636–C648.

Ueshima Y., Yamana H., Sugiyama T., and Ichise E. 1984. Knudsen cell-mass spectrometric study of the thermodynamic properties of Fe-W alloys. *Tetsu to Hagane* 70:549–556.

Wänke H. and Dreibus G. 1986. Geochemical evidence of the formation of the Moon by impact-induced fission of the proto-Earth. In *Origin of the Moon*, edited by Hartmann W. K., Phillips R. J., and Taylor G. J. Houston: Lunar and Planetary Institute. pp. 649–672.

Walker D., Beattie P., and Jones J. H. 1992. Partitioning of U-Th-Pb and other incompatibles between augite and carbonate liquid at 1200 °C and 55 kbar. *Eos* 73:616.

Walter M. J. and Thibault Y. 1995. Partitioning of tungsten and molybdenum between metallic liquid and silicate melt. *Science* 270:1186–1189.

Walter M. J., Newsom H. E., Ertel W., and Holzheid A. 2000. Siderophile elements in the Earth and Moon: Metal/silicate partitioning and implications for core formation. In *Origin of the Earth and Moon*, edited by Canup R. and Righter K. Tucson, Arizona: The University of Arizona Press. pp. 235–289.

Warren P. H. 1985. Origin of howardites, diogenites and eucrites: A mass balance constraint. *Geochimica et Cosmochimica Acta* 49: 577–586.

Warren P. H. 1999. Differentiation of siderophile elements in the Moon and the HED parent asteroid (abstract). 24th Symposium on Antarctic Meteorites. pp. 185–186.

Warren P. H. and Jerde E. A. 1987. Composition and origin of Nuevo Laredo trend eucrites. *Geochimica et Cosmochimica Acta* 51: 713–725.

Wiechert U. H., Halliday A. N., Palme H., and Rumble D. 2004. Oxygen isotope evidence for rapid mixing of the HED meteorite parent body. *Earth and Planetary Science Letters* 221:373–382.